Global NEST Journal, Vol 15, No 2, pp 261-270, 2013

LOCAL SCALE SIMULATION OF AIR TEMPERATURE BY A TWO-STEP HYBRID DOWNSCALING APPROACH USING REGIONAL CLIMATE MODELING AND ARTIFICIAL NEURAL NETWORKS

PHILIPPOPOULOS K.
YIANNIKOPOULOU I.
DELIGIORGI D. *
FLOCAS H.

National and Kapodistrian University of Athens,
Department of Physics,
Division of Environmental Physics and Meteorology
Panepistimioupolis, GR-15784 Athens, Greece

Received: 05/04/13
Accepted: 01/05/13

*to whom all correspondence should be addressed:
e-mail: despo@phys.uoa.gr

ABSTRACT

The influence of microscale and mesoscale meteorology on the local scale variation of air temperature cannot be correctly simulated by the coarse resolution Global Climate Models. The scope of this work is to develop a hybrid dynamic-statistical downscaling procedure and quantify its predictive ability to estimate air temperature variability at finer spatial scales. The study focuses on the warm period of the year (June – August) and the method is applied to eight sites located in Greece with different topographical characteristics. The two-step methodology initially involves the dynamic downscaling of coarse resolution climate data via the RegCM4 regional climate model and subsequently the statistical downscaling of the modeled outputs by training site-specific artificial neural networks (ANN). The RegCM4 model is employed to enhance the representativity of the dataset, while the ANNs are used as function approximators to model the relationship between a number of atmospheric predictor variables and the observed air temperature time series. An insight of the ANN transfer function is obtained by examining the relative contribution of each input variable. The performance of the methodology is evaluated and the results indicate significant improvement from the inclusion of the ANN models in downscaling air temperature.

KEYWORDS: Air temperature, Downscaling, Regional Climate Models, Artificial Neural Networks.

1. INTRODUCTION

Climate modeling is one of the most computationally intensive areas of scientific research and Global Circulation Models (GCMs) are the main tools for assessing climate variability. Their horizontal resolution is roughly 150 km, leading to spatially averaged reconstructions and projections that do not correctly simulate the influence of mesoscale and microscale features on regional or local climate (Pasini, 2008). The requirement for high resolution regional to local scale climate simulations is accomplished by employing dynamical, statistical or dynamic – statistical downscaling models by using the gridded output of GCMs or reanalysis datasets. Dynamical downscaling is performed using Regional Climate Models (RCMs), with their output being dynamically and thermodynamically fully self-consistent while the statistical methods exploit the statistical dependence between the simulated large-scale fields and the climatic variable under study. The dynamical downscaling procedure involves the nesting of a high resolution RCM into the lower resolution GCM (Maraun *et al.*, 2010). RCMs share the same representation of atmospheric physical processes with GCMs but due to their higher spatial and temporal resolution they are able to a more realistic simulation of the regional climate. Climate variability has been studied extensively using RCMs for various regions such as Europe (Giorgi *et al.*, 2004a; b; Raisanen *et al.*, 2004; Gao *et al.*, 2006), North America (Giorgi *et al*, 1994, 1998; Chen *et al.*, 2003; Leung *et al.*, 2004; Diffenbaugh *et al.*, 2005; Duffy *et al.*, 2006), East Asia (Hirakuchi and Giorgi, 1995) and Australia (McGregor and

Walsh, 1994). More recently for the European domain, the PRUDENCE (Christensen and Christensen, 2007; Deque, 2007; Prudence, 2013) and the ENSEMBLES (Hewitt, 2005; "ENSEMBLES", 2013) research projects perform an intercomparison of multiple RCMs driven by several GCMs. Regarding the statistical downscaling methods a wide range of techniques is used, ranging from regression-based to weather generators and weather typing models (Wilby and Wigley, 1997). ANNs are a class of regression-based models and their structure allows them to approximate highly non-linear input-output relationships. In climate downscaling research studies, ANNs have been mainly used for providing local air temperature and precipitation estimations (Coulibali *et al.*, 2005; Moriondo and Bindi, 2006; Haylock *et al.*, 2006; Olsson *et al.*, 2001; Hewitson and Crane; 1996). In a more recent study Chadwick et al. (2011) proposed an ANN approach to downscale ECHAM5 GCM temperature and rainfall fields to a RCM scale with encouraging results. The scope of the current study is to propose a combined dynamic-statistical downscaling procedure for point temperature estimates and test its accuracy in eight meteorological stations with different topographical characteristics.

2. DATA AND METHODS

The climate simulations are performed for the domain presented in Figure 1a and the study utilizes gridded reanalysis datasets and meteorological observations for seven summer periods from 2001 to 2007. The study is focused on June to August when temperature variability is relatively low and extreme temperature climatic conditions (i.e. heat waves) are more frequent, influencing the area of study to a great extent. The selection of the period takes into account the computationally - intensive modeling of the climate system via Regional Climate Models and the requirement of a comprehensive set of training and validation datasets for the ANNs statistical modeling. The seven summer period dataset is considered adequate for examining the performance of the proposed methodology as it consists of 5096 values of three-hourly modeled data. In detail, the four-times daily with a 2.5^{o}x2.5^{o} latitude-longitude horizontal resolution NCEP Reanalysis 2 (NNRP2) dataset (Kanamitsu *et al.,* 2002), containing mean sea level pressure, surface pressure, relative humidity, surface height, air temperature, zonal and meridional wind components. Additionally, mean weekly on a 1-degree spatial resolution Optimum Interpolation Sea Surface Temperatures (OISST) (Reynolds *et al.*, 2002) are used, along with surface air temperature observations from eight meteorological stations in Greece (Figure 1b). The station characteristics are presented in Table 1.

Table 1. Characteristics of meteorological stations

Station	Latitude (°N)	Longitude (°E)	Altitude a.m.s.l. (m)
Kastoria	40.450	21.283	604
Kozani	40.300	21.783	627
Alexandroupoli	40.850	25.917	3
Larissa	39.633	22.417	74
Hellinikon	37.900	23.733	14
Syros	37.417	24.950	72
Tripoli	37.533	22.400	652
Souda	35.483	24.117	151

The selected stations are evenly distributed and cover the topographical characteristics of the area under study. Syros and Souda are island stations, while Alexandroupoli and Hellinikon are representative coastal stations in northeastern and southeastern Greece respectively. Furthermore, Kastoria, Kozani and Tripoli are continental high-altitude stations, whereas Larissa is a characteristic low-altitude mainland station of central Greece.

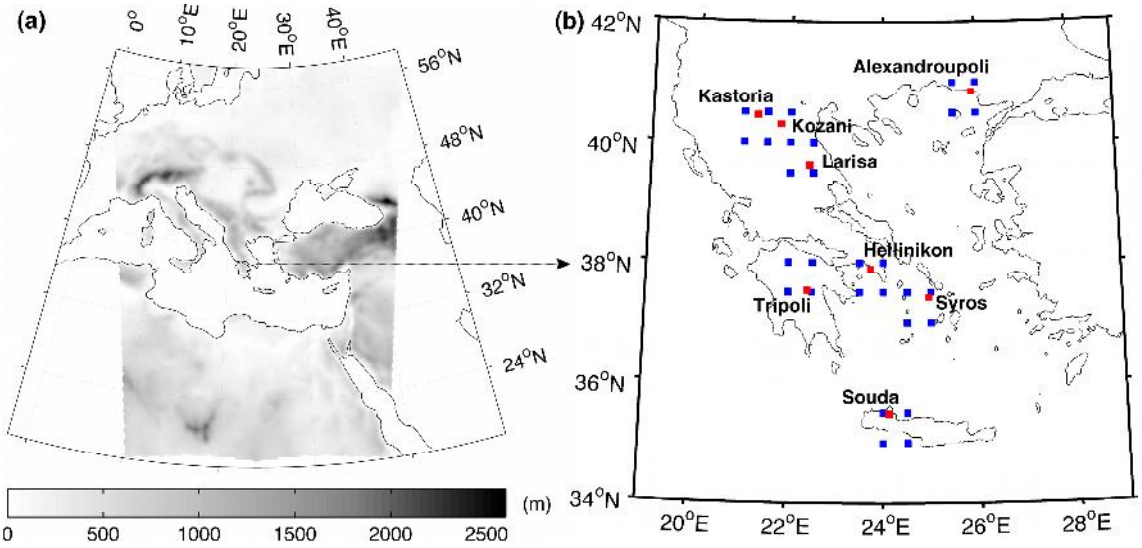

Figure 1. Climate simulations (RegCM4) domain (a) and locations of the meteorological stations (red squares) and of the four nearest RegCM4 grid points for each station (blue squares) (b).

The proposed hybrid downscaling approach consists of two consecutive phases (Figure 2). Initially, gridded climate data are downscaled in a finer spatial scale using the forth version of the ICTP Regional Climate Model (RegCM4) and subsequently its outputs are statistically downscaled at a point location via Artificial Neural Networks (ANN). The model evaluation is based on the comparison between the simulated and observed temperature values at eight selected sites in Greece.

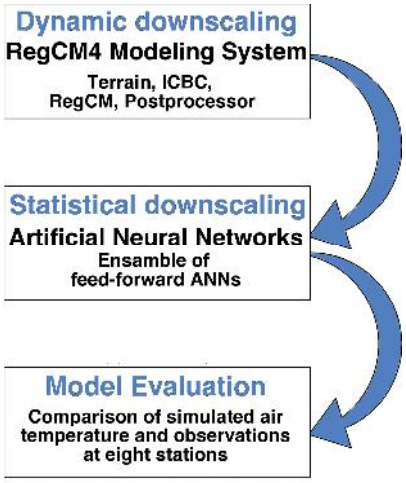

Figure 2. Two-step hybrid downscaling methodology

RegCM4 is a hydrostatic, compressible, sigma-p vertical coordinate model (Giorgi *et al.*, 1993a; Giorgi *et al.*, 1993b) run on an Arakawa B-grid in which wind and thermodynamical variables are horizontally staggered. The RegCM4 model dynamics, which model physics along with the coupling with other components of the climate system, are described thoroughly by Giorgi *et al.* (2012). In this study the NNPR2 and the OISST datasets are used for the reanalysis driven RegCM4 simulations as atmospheric boundary conditions and sea surface temperature input data respectively. The atmospheric component of the model is coupled with the Biosphere-Atmosphere Transfer Scheme BATS (Dickinson *et al.*, 1993) while the subgrid explicit moisture scheme SUBEX (Pal *et al.*, 2000) is used to handle non-convective clouds and precipitation. The RegCM4 domain (Figure 1) in this study is centered at 37.97°N and 23.91°E and consists of 160 points in the longitude and 225 points in the latitude direction, with a 20km horizontal resolution and 18 vertical levels. The output dataset is further postprocessed to produce the three-hourly with a 0.5° spatial resolution regional RegCM4 surface model dataset. For each of the three monthly simulations, a spin-up time of one month (May) is used.

The ANN statistical downscaling scheme is based on the output values of the RegCM4 surface model and in total eight predictor variables (Table 2) are selected for estimating the ambient temperature at local scales. In this study feed forward ANNs are used as function approximators due to their ability of estimating any measurable input-output function to any desired degree of accuracy (Hornik *et al.*, 1989). Feed-forward ANNs are a group of fully directional interconnected neural process elements (PE) and the architecture used in this study, along with the functional model of a single PE is presented in Figure 3. For each station a different ANN is trained and tested for its ability to statistical downscale climate data. The ANNs consist of an input layer with 32 neurons, which are the input nodes of the predictor variables at the four nearest to each target station grid point (Gsw, Gse, Gnw and Gne) and a single neuron in the output layer, which is the output node of the mean three hourly air temperature target values at each station. In each case the selected ANN architecture contains one hidden layer and the number of the hidden layer neurons is determined using the forward selection method. According to this method, an ANN is trained and tested initially using a small number of hidden neurons. Subsequently, the number of hidden neurons is increased and the process is repeated until the results indicate a satisfactory generalization ability of the network (Heaton, 2005). The input–output datasets are divided, using the random sampling approach, into training, validation and test sets, with 70% of the values used for training, 15% for validation and 15% for the test set. The selected percentages (70% -15% -15%) are selected as the optimum configuration since they satisfy the trade-off between the requirement of a representative training dataset and sufficient data for validation and testing. Multiple ANNs are trained with a varying number of hidden layer neurons (from 1 to 70) and the optimum architecture is selected by examining, according to the forward selection method, the Mean Absolute Error (MAE) on the validation set. In all cases, in order to avoid the drawback of the backpropagation algorithm of an initial suboptimal set of weights, training is performed multiple times (25 repetitions).

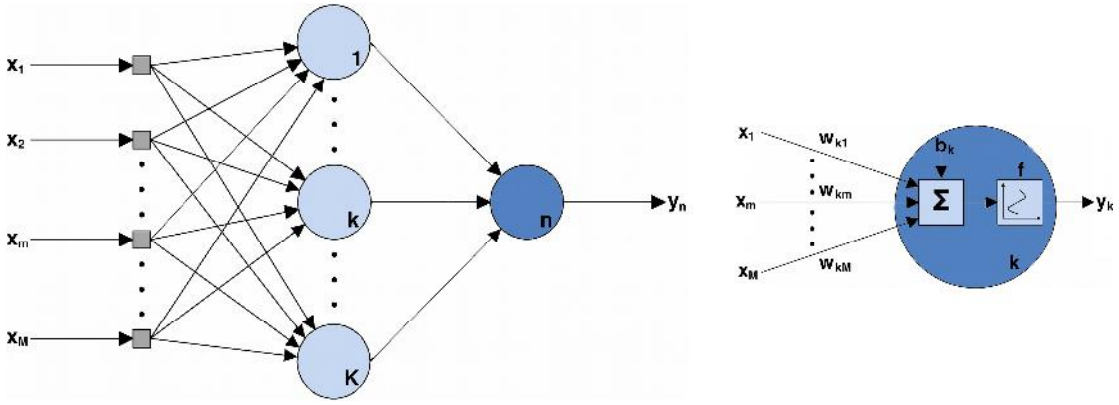

Figure 3. Feed-forward ANN architecture and a single ANN process element

Table 2. RegCM4 surface model output variables, which are used as ANN inputs

	Variable	Description		Variable	Description
1	flw (W m^{-1})	Net longwave	5	sina (W m^{-1})	Solar incident
2	fsw (W m^{-1})	Net solar absorbed	6	t2m (°C)	Temperature (2m)
3	q2m	Specific humidity (2m)	7	u10m (m s^{-1})	Eastward wind (10m)
4	sena (W m^{-1})	Sensible heat	8	v10m (m s^{-1})	Northward wind (10m)

Initially the results of the RegCM4 simulations are directly compared with the land-based observations and subsequently the combined site-specific RegCM4-ANN temperature downscaling procedure is similarly validated versus the station temperature records. An additional comparison is based on the analysis of the results between these two comparisons. The performance evaluation of the proposed downscaling scheme is based on a set of difference and correlation measures (Willmott, 1982). The results of the MAE, the Root Mean Square Error (RMSE), the Mean Bias Error (MBE), the Mean Absolute Percentage Error (MAPE), the correlation coefficient (R), the coefficient of determination (R^2) and the index of agreement (d) are discussed and the scatter diagrams of the observed versus the predicted values are presented for each station. Furthermore, the residuals,

which represent the portion of the test data that are not explained by the downscaling methodology, are analyzed by examining their distributions.

An insight into the underlying input-output transfer function of the statistical downscaling element of the methodology is obtained by utilizing the weights method (Garson, 1991). The method determines the relative importance (RI) of the predictor variable inputs in estimating air temperature for each station. The method is commonly used for identifying the optimum set of inputs in neural networks and it involves the partitioning of the hidden-output layer weights of each hidden neuron in components that are associated with each input neuron.

3. RESULTS AND DISCUSSION

An initial analysis of the RegCM4 simulation results is performed by comparing the observed temperature values at the eight target stations against the corresponding simulated values at the four nearest to each station grid points. The analysis reveals the grid point that is more closely related to the station observations. An interesting remark is that for half of the stations (Alexandroupoli, Hellinikon, Syros and Tripoli) the lower MAE values are not observed for the most geographically proximate to the station grid point (Table 3). This finding is further established from the comparison of the observed and simulated air temperature distributions by plotting the corresponding box-plots (Figure 4). A characteristic case is illustrated for the Tripoli site where the most proximate grid point (Gse) systematically overestimates air temperature (3.08°C MAE value), while the most distant point (Gnw) reproduces the observed temperature distribution with more accuracy (Figure 4g), a finding related to the complex topographical features of the region. On the contrary, an example of a good agreement between the closest to the station grid point and in-situ observations is noted at the Souda site where the Gnw point is similar to the station air temperature distribution (Figure 4h) with a relative low MAE value (1.68°C).

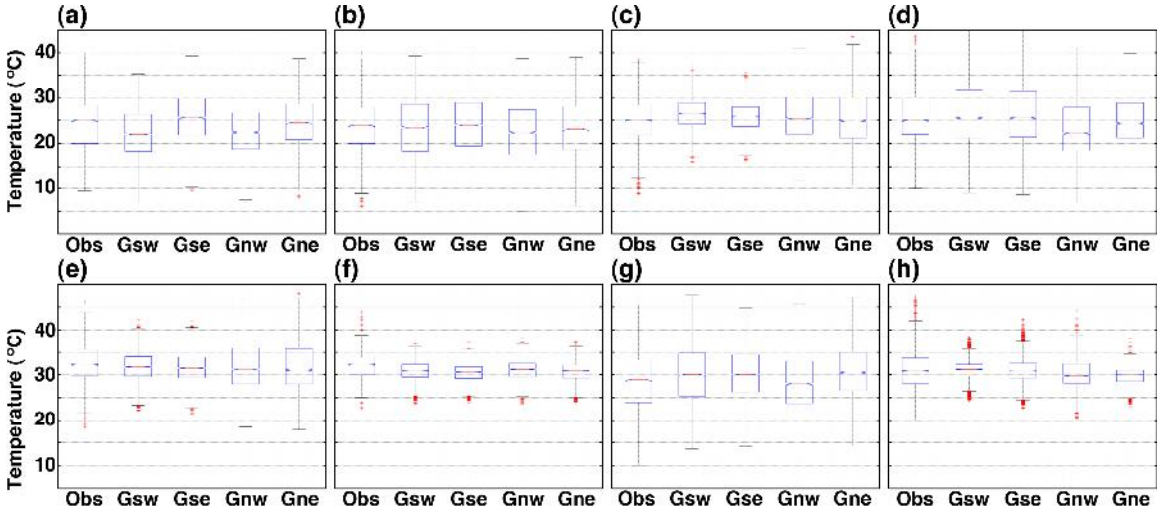

Figure 4. Box-plots comparison of the observed and RegCM4 simulated temperature at the four closest grid points at Kastoria (a), Kozani (b), Alexandroupoli (c), Larissa (d), Hellinikon (e), Syros (f), Tripoli (g) and Souda (h)

According to the results of Table 3, better agreement is observed for the island stations (Souda and Syros) whereas there are considerable discrepancies for the inland, high altitude stations (Tripoli, Kastoria and Kozani). The MAE values range from 1.68 °C to 3.08 °C for the Souda and Tripoli station respectively. Regarding Alexandroupoli and Souda sites, higher errors are observed when comparing the grid points located over sea with the land-based station data. This is attributed to the different ambient temperature characteristics prevailing over sea and soil.

Table 3. MAE results in °C between temperature observations and RegCM4 grid points. Boldfaced values correspond to the errors of the closest to the station grid point

	Kastoria	Kozani	Alexandroupoli	Larissa	Hellinikon	Syros	Tripoli	Souda
Gsw	3.45	2.69	2.23	2.49	1.73	1.69	3.25	2.37
Gse	3.06	2.50	2.19	**2.18**	1.72	1.93	3.08	1.80
Gnw	3.22	2.85	2.13	3.29	**2.24**	1.48	**2.90**	**1.68**
Gne	**2.77**	**2.43**	**2.25**	2.21	2.28	**1.74**	3.15	3.38

An insight of the in-situ observations versus the simulated temperature values at the grid point with the better agreement in terms of the overall MAE, is presented in the scatter diagrams of Figure 5. Significant dispersion along the optimum agreement line is observed and RegCM4 simulation biases are evident even for stations with relatively low MAE values. In detail, RegCM4, clearly overestimates high temperature values in Hellinikon, Syros and Souda (Figure 5e, 5f and 5h), while for the Alexandroupoli station the opposite phenomenon is observed (Figure 5c). Although for the remaining of the stations there is no evident bias, significant dispersion is observed.

This under-representation of local ambient temperature highlights the importance of incorporating sophisticated statistical models as post-processing elements of regional climate models. The ANNs in this study are selected for their characteristic ability to model nonlinear relationships between predictors and predictands, a feature highly desirable for modeling the non-linear climate system. According to the proposed methodology, 1,750 different ANNs are trained and tested for each station and the optimum architecture (number of input, hidden and output neurons) is presented in each case in Table 4. A general remark is that for the mainland coastal (Alexandroupoli and Hellinikon) and for the island stations (Syros and Souda) the number of hidden layer neurons is smaller compared to the inland stations. This finding can be attributed to the reduced complexity of the input-output mapping, accomplished by the ANN transfer function.

Table 4. Number of input, hidden and output layer neurons

	Kastoria	Kozani	Alexandroupoli	Larissa	Hellinikon	Syros	Tripoli	Souda
Input	32	32	32	32	32	32	32	32
Hidden	69	50	45	67	39	41	58	43
Output	1	1	1	1	1	1	1	1

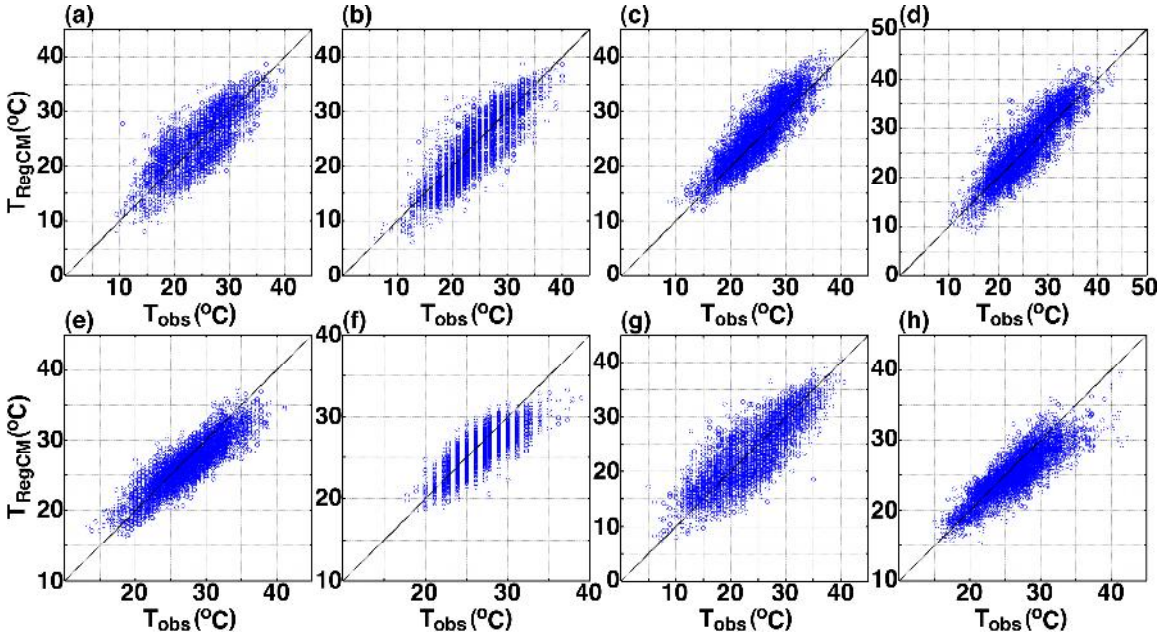

Figure 5. Comparison scatter plots between RegCM4 simulated temperature and observations at Kastoria (a), Kozani (b), Alexandroupoli (c), Larissa (d), Hellinikon (e), Syros (f), Tripoli (g) and Souda (h)

The overall results of the methodology are presented in Table 5 and the scatter diagrams of the observed versus the predicted air temperature values for all stations in Figure 6. The low dispersion along the optimal agreement line illustrates the ability of the methodology to sufficiently model the effects of local topography in air temperature variation. In detail, the explained variance of the ambient temperature by the proposed downscaling procedure is greater than 87% for all stations and up to 90% for the Souda and Alexandroupoli sites. The best results are obtained for the Syros and Souda stations with 0.83 °C and 0.87 °C MAE values respectively and less than 3.5% MAPE values. Relatively higher errors are obtained for the inland stations and especially for the Tripoli site (1.41 °C) The method in general does not systematically over- or under-estimate the observed temperature values, exhibiting minor MBE values for all stations except Kastoria and Kozani. The latter stations show evidence of slight overestimation and underestimation with 0.28 °C and -0.15 °C MBE values respectively. This finding is consistent with the residual distributions (Figure 7) which are centered for all stations at the [-0.75, 0.75] interval. Specifically for the best performing sites (Syros and Souda) the distributions are centered with high relative frequencies around 0 °C at the [-0.5, 0.5] interval (Figure 7f and 7h).

Table 5. Model evaluation results

	MAE (°C)	RMSE (°C)	MBE (°C)	MAPE (%)	*R*	R^2	d
Kastoria	1.24	1.94	0.28	5.43	*0.94*	0.87	0.97
Kozani	1.28	1.90	-0.15	5.48	*0.93*	0.87	0.96
Alexandroupoli	1.13	1.47	0.08	4.83	*0.95*	0.90	0.97
Larissa	1.22	1.79	-0.04	5.07	*0.95*	0.89	0.97
Hellinikon	1.05	1.35	0.00	3.96	*0.95*	0.89	0.97
Syros	0.83	1.09	0.07	3.06	*0.92*	0.85	0.96
Tripoli	1.41	2.14	0.06	6.65	*0.94*	0.88	0.97
Souda	0.87	1.23	0.01	3.42	*0.95*	0.90	0.97

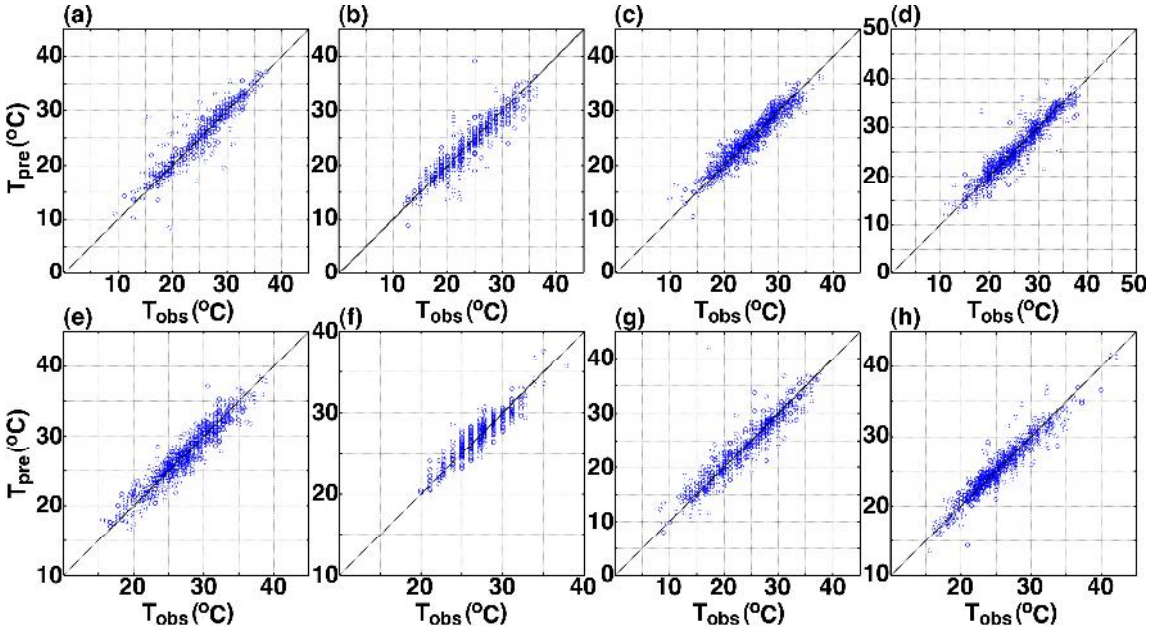

Figure 6. Comparison of the downscaled air temperature and observations at Kastoria (a), Kozani (b), Alexandroupoli (c), Larissa (d), Hellinikon (e), Syros (f), Tripoli (g) and Souda (h)

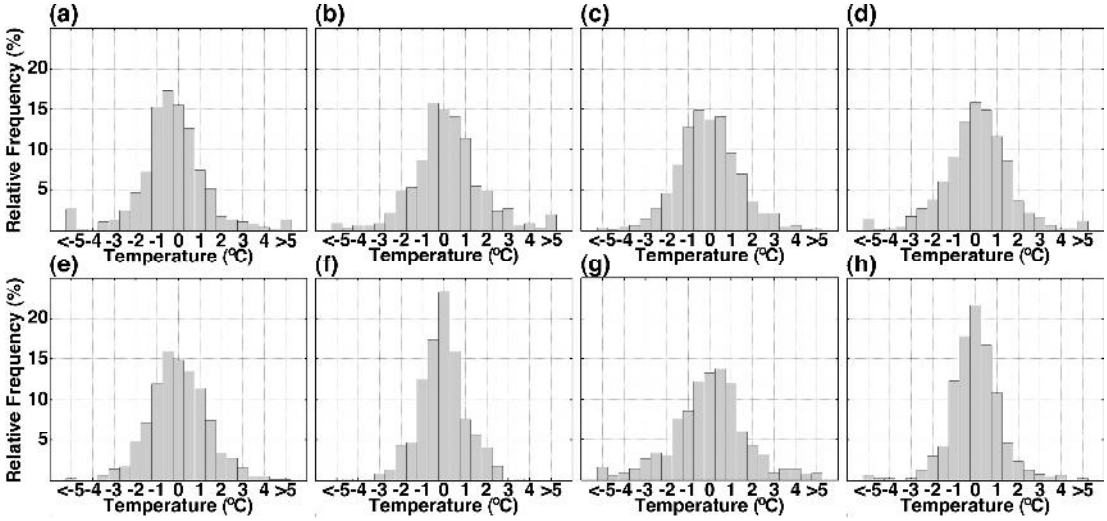

Figure 7. Residual distributions at Kastoria (a), Kozani (b), Alexandroupoli (c), Larissa (d), Hellinikon (e), Syros (f), Tripoli (g) and Souda (h)

The inclusion of the statistical element of the downscaling procedure results in significant improvement in terms of the overall test set MAE. The relative MAE decreases range from 46% to 55.8% for the Larissa and Tripoli stations respectively. Higher decreases are observed for the stations where the RegCM4 simulations exhibited the highest errors.

The relative contribution of each predictor variable from the application of the weights method, averaged over all grid points, is presented in Figure 8. The results denote the relevance of the selected predictors in estimating ambient temperature. In general, two different patterns are observed. According to the first pattern (Kozani, Hellinikon and Syros) the net solar absorbed radiation (fsw) and solar incident (sina) variables contribute less to a certain extent, while the modeled output of sensible heat (sena), temperature (T) and net longwave (flw) exhibit the higher RI values. According to the second pattern, no significant differences between the variables' RI are observed, a finding that is more evident at the Larissa and Tripoli stations.

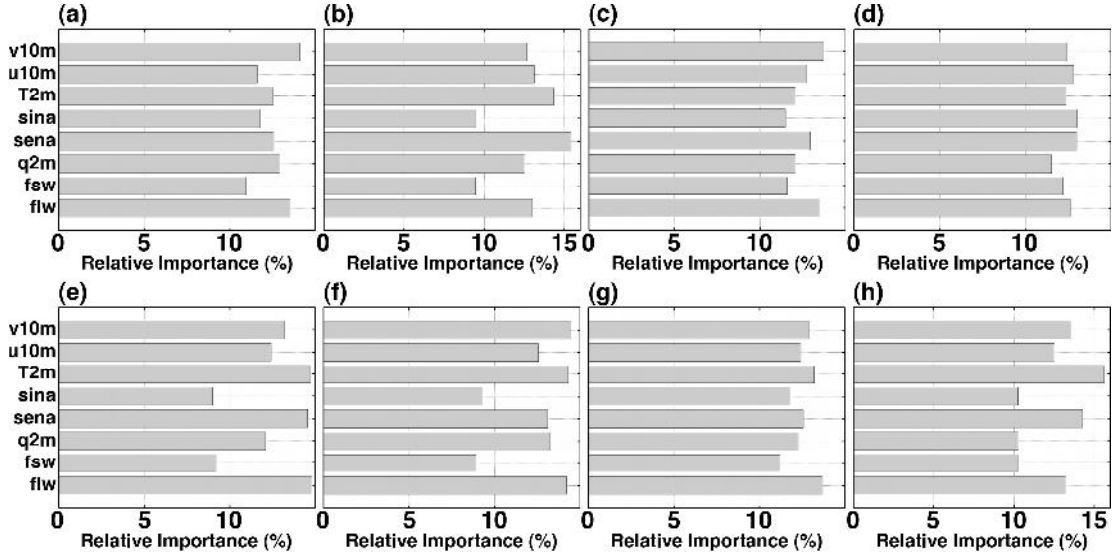

Figure 8. Relative importance of ANN input parameters at Kastoria (a), Kozani (b), Alexandroupoli (c), Larissa (d), Hellinikon (e), Syros (f), Tripoli (g) and Souda (h)

4. CONCLUSIONS

This work highlights the importance of combining dynamic and statistical downscaling models for effectively estimating meteorological variables in local scales. The selected RegCM4-ANN downscaling method gives promising results for providing site-specific ambient temperature values, especially for the mainland coastal and island sites. An advantage of including a statistical downscaling element in the downscaling procedure is their ability to provide on-site climate information; this is highly desirable in climate impact studies and policy making and can be achieved by training different site-specific ANNs for targeted locations. The statistical element of the methodology (ANNs) can be extended to include not only the RegCM4 surface outputs but also large-scale GCM or reanalysis data predictors. Future work is suggested for estimating the uncertainties and the related errors of regional climate models driven by GCMs for the Eastern Mediterranean and selecting the optimum statistical downscaling procedure for more reliable future projections of climate change at finer spatial scales.

AKNOWLEDGEMENTS

This research has been co-funded by the European Union and Greek national funds through the Operational Program "Education and Lifelong Learning" of the National Strategic Reference Framework (NSRF) – Research Funding Program: Heraclitus II: Investing in knowledge society through the European Social Fund.

REFERENCES

Chadwick R., Coppola E. and Giorgi F. (2011), An artificial neural network technique for downscaling GCM outputs to RCM spatial scale, *Nonlin Processes Geophys*, **18**, 1013-1028.

Chen M., Pollard D. and Barron E.J. (2003), Comparison of future climate change over North America simulated by two regional models, *J Geophys Res,* **108**, 4348.

Christensen J.H. and Christensen O.B. (2007), A summary of the PRUDENCE model projections of changes in European climate by the end of this century, *Climatic Change*, **81**, 7–30.

Coulibaly P., Dibike B.Y. and Anctil F. (2005), Downscaling Precipitation and Temperature with Temporal Neural Networks, *J Hydrometeor*, **6**, 483–496.

Deque M. (2007), Frequency of precipitation and temperature extremes over France in an anthropogenic scenario: Model results and statistical correction according to observed values, *Global Planet Change,* **57**, 16-26.

Dickinson R.E., Henderson-Sellers A., Kennedy P.J. (1993), Biosphere-Atmosphere Transfer Scheme (BATS) version 1e as coupled to the NCAR Community Climate Model. Natl Cent for Atmos Res, Boulder.

Diffenbaugh N.S., Pal J.S., Trapp R.J. and Giorgi F. (2005), Fine-scale processes regulate the response of extreme events to global climate change, *P Natl Acad Sci USA*, **102**, 15774–15778.

Duffy P.D., Arritt R.W., Coquard J., Gutowski W., Han J., Iorio J., Kim J. Leung L.R., Roads J. and Zeledon E. (2006), Simulations of present and future climates in the western United States with four nested regional climate models, *J Climate,* **19**, 873–895.

ENSEMBLES (April 2013), *ensembles-eu.org*

Gao X., Pal J.S. and Giorgi F. (2006), Projected changes in mean and extreme precipitation over the Mediterranean region from a high resolution double nested RCM simulation, *Geophys Res Lett*, **33**, L03706.

Garson G.D. (1991), Interpreting neural-network connection weights, *AI Expert,* **6**, 47-51.

Giorgi F., Marinucci M.R., Bates G.T. (1993a), Development of a second generation regional climate model (RegCM2) I: Boundary layer and radiative transfer processes, *Mon Wea Rev,* **121**, 2794-2813.

Giorgi F., Marinucci M.R., Bates G.T. (1993b), Development of a second generation regional climate model (RegCM2) II: Convective processes and assimilation of lateral boundary conditions, *Mon Wea Rev*, **121**, 2814-2832.

Giorgi F., Shields C. and Bates G.T. (1994), Regional climate change scenario over the United States predicted with a nested regional climate model, *J Climate*, **7**, 375–399.

Giorgi F., Mearns O., Shields C. McDaniel L. (1998), Regional nested model simulations of present day and 2 x CO_2 climate over the central plains of the U.S., *Climatic Change*, **40**, 457–493.

Giorgi F., Xunquiang B. and Pal J.S. (2004a), Mean interannual variability and trends in a regional climate change experiment over Europe. I: Present-day climate (1961–1990), *Clim Dynam*, **22**, 733–756.

Giorgi F., Xunquiang B. and Pal J.S. (2004b), Mean interannual variability and trends in a regional climate change experiment over Europe. II: Climate change scenarios (2071–2100), *Clim Dynam*, **23**, 839–858.

Giorgi F., Coppola E., Solmon F., Mariotti L., Sylla M.B., Bi X., Elguindi N., Diro G.T., Nair V., Giuliani G., Turuncoglu U.U., Cozzini S., Güttler I., O'Brien T.I., Tawfik A.B., Shalaby A., Zakey A.S., Steiner A.L., Stordal F., Sloan L.C and Brankovic C. (2012), RegCM4: model description and preliminary tests over multiple CORDEX domains, *Clim Res*, **52**, 7-29.

Haylock M. R., Cawley, G.C., Harpham C. Wilby R.L. and Goodess C.M. (2006), Downscaling heavy precipitation over the United Kingdom: a comparison of dynamical and statistical methods and their future scenarios, *Int J Climatol*, **26**(10), 1397-1415.

Heaton J. (2005), Introduction to neural networks with Java. 1st edn. Heaton Research Inc., Chesterfield.

Hewitson B. and Crane R. (1996), Climate downscaling: techniques and application, *Clim Res*, **7**, 85-95.

Hewitt C. (2005), The ENSEMBLES Project—Providing ensemble-based predictions of climate changes and their impacts, *EGU Newsletter*, **13**, 22–25.

Hirakuchi H. and Giorgi F. (1995), Multi-year present and 2 x CO_2 simulations of monsoon climate over Asia and Japan with a regional climate model nested in a general circulation model, *J Geophys Res,* **100**,105–126.

Hornik K., Stinchcombe M. and White H. (1989), Multilayer feedforward networks are universal approximators, *Neural Networks,* **2**, 359-366.

Kanamitsu M., Ebisuzaki W., Woollen J., Yang S., Hnilo J.J., Fiorino M. and Potter G.L. (2002), NCEP-DEO AMIP-II Reanalysis (R-2), *Bul of the Atmos Met Soc,* **83**, 1631-1643.

Leung L. Qian R.Y., Bian X., Washington W.M., Han J. and Roads J.O. (2004), Mid-century ensemble regional climate change scenarios for the western United States, *Climatic Change*, **62**, 75–113.

Maraun D., Wetterhall F., Ireson A.M., Chandler R.E., Kendon E.J., Widmann M., Brienen, S., Rust H.W., Sauter T., Themeßl M., Venema V.K.C., Chun K.P., Goodess C.M., Jones R.G., Onof C., Vrac M. and Thiele-Eich I. (2010), Precipitation downscaling under climate change: Recent developments to bridge the gap between dynamical models and the end user, *Rev. Geophys.*, **48**(3), RG3003.

McGregor J.L. and Walsh K. (1994), Climate change simulations of Tasmanian precipitation using multiple nesting, *J Geophys Res*, **99**, 20889–20905.

Moriondo M. and Bindi M. (2006), Comparison of temperatures simulated by GCMs, RCMs and statistical downscaling: potential application in studies of future crop development, *Clim Res*, **30**, 149-160.

Olsson J., Uvo C.B., Jinno K. (2001), Statistical atmospheric downscaling of short-term extreme rainfall by neural networks, *Phys Chem Earth Part B*, **26**(9), 695-700.

Pal J.S., Small E.E., Eltahir E.A.B. (2000), Simulation of regional scale weather and energy budgets: representation of sub-grid cloud and precipitation processes within RegCM, *J Geophys Res,* **105**, 29579-29594.

Pasini A. (2008), Neural Network Modeling in Climate Change Studies, In: Haupt SE, Pasini A, Marzban C (ed) Artificial Intelligence Methods in the Environmental Sciences, 1st edn. Springer.

Prudence (2013) Prediction of Regional scenarios and Uncertainties for Defining EuropeaN Climate change risks and Effects, *prudence.dmi.dk*

Raisanen J., Hansson U., Ullerstig A., Döscher R., Graham L.P., Jones C., Meier H.E.M., Samuelsson P. and Willen U. (2004), European climate in the late twenty-first century: Regional simulations with two driving global models and two forcing scenarios, *Clim Dynam*, **22**, 13–31.

Reynolds R.W., Rayner N.A., Smith T.M., Stokes D.M. and Wang W. (2002), An improved in situ and satellite SST analysis for climate, *J Climate*, **15**, 1609-1625.

Wilby R.L. and Wigley T.M.L. (1997), Downscaling general circulation model output: a review of methods and limitations, *Prog Phys Geogr*, **21**, 530-548.

Willmott C.J. (1982), Some comments on the evaluation of model performance, *Bull Amer Meteor Soc,* **63**, 1309-1313.